CSMA 2024
16ème Colloque National en Calcul des Structures
13-17 Mai 2024, Presqu'île de Giens (Var)

A multi-scale model for fast HCF characterization of alloys in the presence of process-induced defects

Abhishek Palchoudhary[1], Cristian Ovalle[1], Vincent Maurel[1], Pierre Kerfriden[1]

[1] *MINES Paris, PSL University, Centre des Matériaux (CMAT), CNRS UMR 7633, BP 87 91003 Evry, France, abhishek.palchoudhary@minesparis.psl.eu*

Résumé — The presence of process-induced meso-scale pores, typically present in a variety of cast and additively manufactured alloys, typically leads to a low fatigue limit and an important dispersion related to the distribution of pores. On the other hand, a scatter in fatigue life still exists due to inherent micro-structural heterogeneity like silicon precipitates in the matrix in between pores. Therefore, a new fatigue model modelling uncertainty on two scales, i.e. due to varying pore distributions and micro-structural heterogeneity is proposed. A stochastic approach for the micro-plasticity based on a separation of scales is chosen to model uncertainty due micro-structural heterogeneity, and a weakest link assumption is applied to extend this theory to incorporate uncertainty due to varying distribution of pores. The finite element method is used to take into account the complex morphology of pores, and a previously implemented Neuber-type method was used for fast approximation of the full-field elasto-plastic stresses in porous structures. The parameters of the multi-mechanism model are obtained via a maximum likelihood estimate using tomography-based randomly generated synthetic porous specimens on experimental fatigue data.

Mots clés — Multi-scale approach, Probabilistic fatigue lifetime modelling, Pores, Size effect.

1 Introduction

Certain metals, owing to their fabrication process, end up with defects at two scales, notably meso-scale pores which can have high effective sizes and complex shapes, and inherent micro-heterogeneity due to inclusions and varying grain orientations. Examples of these materials include foundry alloys (Al-Si) [1], additive manufacturing alloys, which often contain keyhole pores, lack of fusion pores, [2] etc. Both microstructural factors (presence of eutectics, etc.) as well as pore characteristics that cause high stress concentrations (such as the pore density, size, shape and distance to the surface) play an important role in final failure, and therefore bring about an important dispersion in the fatigue lifetime. In this light, engineering decisions on the usability of such porous material for structural use need a model that is both fast to use, easy to calibrate and provides uncertainty estimates in the lifetimes.

The micro-inclusion model [3, 4, 5] has been directly applied for probabilistic fatigue modelling of a wide range of metallic alloys that are relatively homogeneous, i.e. without the presence of large pores that bring about high stress concentrations [3, 4, 6, 7, 8]. However, this approach is not directly applicable to porous specimens which contain heterogeneous stresses. There exist a few approaches to take this into account, which include an indirect approach that does not explicitly model the pores [5, 9] and another approach to incorporate the effect of isolated spherical pores [10].

In this paper, a probabilistic fatigue model is developed that takes into account lifetime dispersion due to defects at two scales. The first section is dedicated to the methodology, which recalls the formal description of the micro-inclusion model for homogeneous stress cases and the development of the two-scale probabilistic model for heterogenous stress cases, followed by synthetic specimen generation for calibration of the model. The second section is devoted to numerical results of the model.

2 Methodology

2.1 Material

For this study, a porous Al-Si7Mg0.3 alloy was considered. This alloy has been subject to a lot of studies, and their microstructure and distribution of pores, as well as their elasto-plastic behavior is known [1, 11]. The pores consist of shrinkage and gas pores, which originate from the manufacturing process of lost wax casting. Fatigue experiments in the high-cycle fatigue regime, under alternating tension-compression conditions with zero mean stress, have previously been carried out on this alloy in [1].

2.2 Micro-inclusion model

The micro-inclusion model [3, 4] operates on an assumption of separation of scales. It assumes that fatigue lifetime of a homogeneously loaded structure, as observed at the macro scale, is governed by an underlying stochastic damaging process at the micro-scale. A Poisson process is assumed for the appearance of micro-inclusions in a volume that follow a kinematic hardening law beyond their yield stresses. The intensity of their appearance is a power law of the applied stress amplitude, and the weakest link hypothesis is used to describe rupture, which leads to a Weibull distribution of the yield stress of the weakest inclusion. A criteria based on a critical value of accumulated plastic strain for the weakest site governs the micro fatigue life [5]. While several fatigue lifetime criteria exist, this paper will use a criteria based on a critical value of cumulated plastic strain for a site, that is considered to govern the fatigue life in a given volume. [5, 12] A brief description of the model is given as follows :

In a given volume V, the number of active microplastic sites X, which are seen as elasto-plastic inclusions, is modelled as a random variable, and follows a Poisson process with intensity Λ :

$$\text{Prob}(X = k) = \frac{(\Lambda)^k}{k!} \exp(-\Lambda) \tag{1}$$

The intensity of the Poisson process Λ is assumed to be a power law of the stress Σ_0 experienced by the volume V :

$$\Lambda(\Sigma_0; m, \beta, V) = \frac{V}{\beta} (\Sigma_0)^m \text{ where } \beta = V_o S_o^m \tag{2}$$

where m and β are parameters of the model that govern the relation between the intensity of the process and the stress.

A weakest link assumption is applied, i.e. the weakest site should govern the fatigue life. Each site can be considered to have a yield stress σ_y^{site}, and the yield stress of the weakest site is given by Σ_∞ which is modelled as a random variable :

$$\Sigma_\infty = \min_{sites} \sigma_y^{site} \tag{3}$$

In doing so, one express the probabilities in terms of yield stress of the weakest inclusion Σ_∞ instead of the number of active sites :

$$\text{Prob}(\exists \geq 1 \text{ site with } \sigma_y^{site} < \Sigma) = \text{Prob}(\Sigma_\infty < \Sigma) = F_{\Sigma_\infty}(\Sigma) \tag{4}$$

Thus, the distribution function of the yield stress of the weakest site as a function of the experienced stress Σ_0 becomes a 2-parameter Weibull with a a scale parameter m and a shape parameter given as :

$$\lambda(V; m, \beta) = \left(\frac{\beta}{V}\right)^{1/m} \tag{5}$$

$$F_{\Sigma_\infty}(\Sigma;m,\beta) = 1 - \exp\left(-\left(\frac{\Sigma}{\lambda(V;m,\beta)}\right)^m\right) \tag{6}$$

With the density expressed as the derivative :

$$f_{\Sigma_\infty}(\Sigma;m,\beta) = \frac{m}{\lambda(V;m,\beta)}\left(\frac{\Sigma}{\lambda(V;m,\beta)}\right)^{m-1}\exp\left(-\left(\frac{\Sigma}{\lambda(V;m,\beta)}\right)^m\right) \tag{7}$$

To express this density in terms of the number of cycles to failure N_R, a criterion [5] that considers crack initiation and rupture to be governed by a critical value of accumulated plasticity in the weakest micro-inclusions [12] is taken. The fatigue lifetime is considered to be finite if the weakest inclusion has a yield stress less than the stress experienced by the loaded volume, and infinity otherwise. Owing to the probabilistic nature of the appearance of the weakest inclusion, the fatigue lifetime is also probabilistic, and is modelled as a random variable :

$$N_R = \begin{cases} \frac{A}{(\Sigma_0-\Sigma_\infty)^2}, & \text{if } \Sigma_\infty < \Sigma_0 \\ +\infty, & \text{if } \Sigma_\infty \geq \Sigma_0 \end{cases} \tag{8}$$

The lifetime density function $f_{N_R}(N)$ is obtained via a change of variables. We define :

$$g(\Sigma_\infty;A,\Sigma_0) = \frac{A}{(\Sigma_0-\Sigma_\infty)^2} \tag{9}$$

$$g^{-1}(N;A;\Sigma_0) = \Sigma_0 - \sqrt{\frac{A}{N}} \tag{10}$$

$$f_{N_R}(N;m,\beta,A,\Sigma_0) = \begin{cases} (f_{\Sigma_\infty}(\Sigma;m,\beta)\circ g^{-1}(N;A,\Sigma_0))\left.\frac{dg^{-1}}{dN}\right|_N & \\ +\text{Prob}(\Sigma_\infty > \Sigma_0|m,\beta)\delta_{N_R=\infty}(N), & \text{if } N > \frac{A}{\Sigma_0^2} \\ 0, & \text{if } N \leq \frac{A}{\Sigma_0^2} \end{cases} \tag{11}$$

And the lifetime distribution function is obtained by integration of the density function :

$$F_{N_R}(N;m,\beta,A,\Sigma_0) = \begin{cases} \left[1-\exp\left(-\frac{g^{-1}(N;A,\Sigma_0)}{\lambda(V;m,\beta)}^m\right)\right] & \\ +\text{Prob}(\Sigma_\infty > \Sigma_0|m,\beta)H_{N_R=\infty}(N), & \text{if } N > \frac{A}{\Sigma_0^2} \\ 0, & \text{if } N \leq \frac{A}{\Sigma_0^2} \end{cases} \tag{12}$$

$$\text{Where } H_{N_R=a}(N) = \begin{cases} 1, & \text{if } N > a \\ 0, & \text{if } N \leq a \end{cases} \tag{13}$$

$$\text{Prob}(\Sigma_\infty > \Sigma_0|m,\beta) = \exp\left(-\left(\frac{\Sigma_0}{\lambda(V;m,\beta)}\right)^m\right) \tag{14}$$

The set of parameters thus introduced is summarized as :

$$\mu = [m,\beta,A] \tag{15}$$

Later on, the dependence of f_{N_R} and F_{N_R} on μ will be introduced as $f_{N_R}(N;\mu,\Sigma_0)$ and $F_{N_R}(N;\mu,\Sigma_0)$

2.3 Two-scale probabilistic fatigue model

It is desired to model the life of a structure containing gradients of stresses arising due to its geometry (specifically, pores). The micro-inclusion model can thus remain valid in the matrix between the pores, as long as the local loading rests elastic (a correction of elastic stresses [13] or inclusion of a mixed model incorporating plasticity is required otherwise). This is shown schematically in 1. A finite element method is used to explicitly mesh structures with pores (an example is shown in Figure 2). These are linear elements with piece-wise constant approximation of the stresses. The life of such a structure is dependent on the finite elements that constitute it. The stress experienced by each finite element is constant per element. Thus, the probability of the failure of the structure (modelled by the random variable N_R^s) can be obtained via a weakest link assumption at the level of its linear finite elements (denoted by e) :

$$\text{Prob}(N_R^s \leq N) = 1 - \prod_e (1 - \text{Prob}(N_R^e < N)) \tag{16}$$

$$F_{N_R^s}(N;\mu,\Sigma_a) = 1 - \prod_e (1 - F_{N_R}(N;\mu,\Sigma_0^e(\Sigma_a)) \tag{17}$$

Where $\Sigma_0^e(\Sigma_a)$ is a function that gives, for an applied loading Σ_a on the porous structure, the loading Σ_0^e experienced (a corrected equivalent Von-Mises stress amplitude in the stabilized cycle, calculated via a fast plastic corrector developped in [13] is taken) by each element e in the structure via the Finite Element Method. The probability density of failure of the structure is obtained via perturbation of the distribution function (where ε is a small perturbation parameter) :

$$f_{N_R^s}(N;\mu,\Sigma_a) \approx \frac{1}{\varepsilon}\left(F_{N_R^s}(N+\varepsilon;\mu,\Sigma_a) - F_{N_R^s}(N;\mu,\Sigma_a)\right) \tag{18}$$

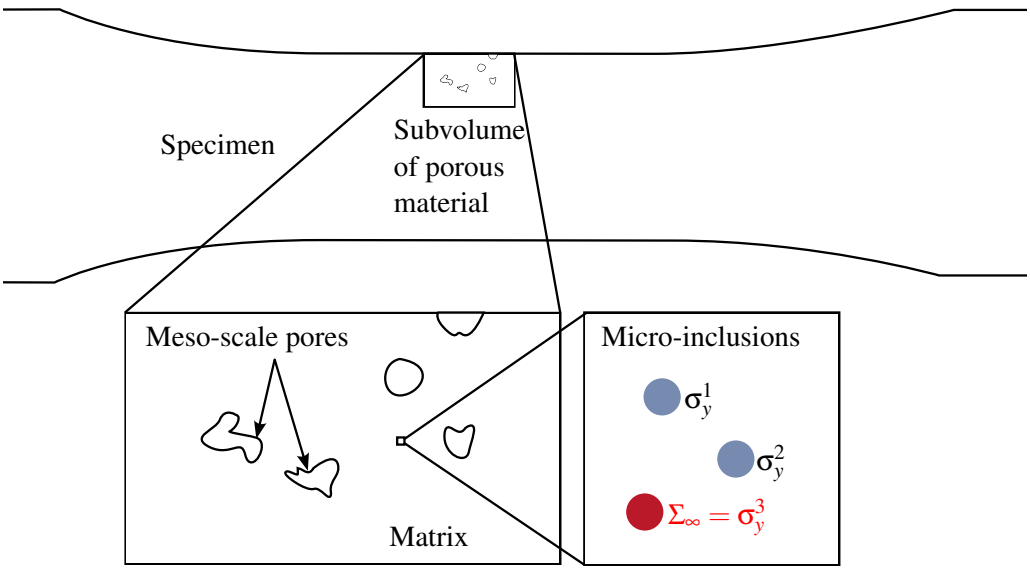

FIGURE 1 – Example of a specimen containing a sub-volume of pores, with the micro-inclusion model activating in the matrix between the pores

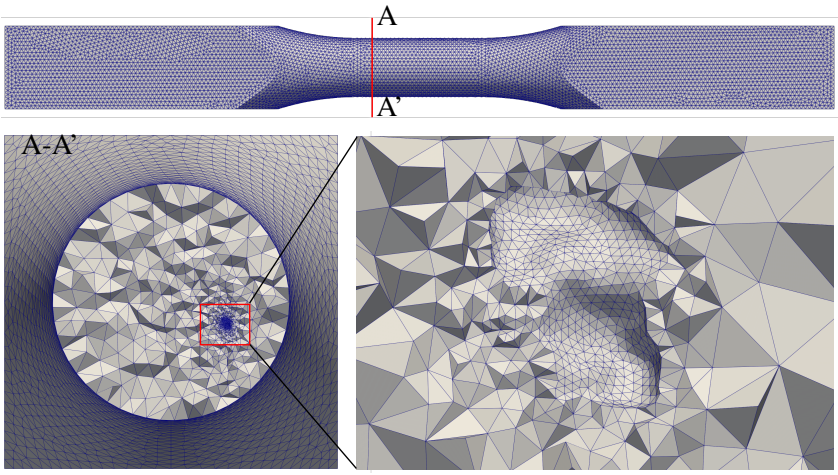

FIGURE 2 – Example of a specimen containing a sub-volume of pores as a finite element mesh, with a zoom of the mesh around a pore

2.4 Generation of synthetic porous specimens

Fatigue experiments that were carried out in [1] used a particular cylindrical geometry of specimens. Tomographies of these specimens were not available, therefore, $12 \times 13 \times 3\text{mm}^3$ regions of planar specimens were tomographied to obtain information about the distribution of pores present in alloy C. These pores were segmented based on a threshold on contrast, remeshed to obtain surface meshes, and filtered to remove small defects known not to affect the fatigue life [11, 14, 15]. The volume of the cylindrical fatigue specimens, being around 589mm^3, contains a very large number of defects even with the size filtering, and as such, needs to be split up to pass in memory for Finite Element calculations. Therefore, the following steps were done to simulate a synthetic porous specimen :

— 100 cylindrical specimens with the geometry of the specimens used for the fatigue experiments were created, and these specimens were populated with subvolumes of pores taken from the pool of filtered defects, each subvolume being $1/20^{\text{th}}$ the size of the specimen

— Elastic calculations were performed on the 100 specimens each containing one subvolume of pores

— The equivalent Von-Mises stress amplitudes in the stabilized cycle (corrected for plasticity via a fast plastic corrector developped in [13]) and volumes associated to the elements in the subvolumes were extracted. A random combination of 20 such subvolumes are considered to make up one synthetic porous specimen. Examples of synthetically generated porous specimens are shown in 3.

2.5 Parameter identification

For the purposes of this paper, identification of all parameters will be done exclusively on available experimental fatigue data, via a maximum likelihood estimate. This requires a likelihood function, which, when maximized, will output parameters $\mu = [m, \beta, A]$ of the lifetime model that are the most probable given the experimental fatigue results. If I is the set of all the experimental specimens tested for fatigue failure, and $\mathcal{K}$ is the set of all possible synthetic porous specimens, the likelihood is calculated as :

$$\mu = \arg\max_{\tilde{\mu}} \mathop{\mathbb{E}}_{k \in \mathcal{K}} \left(\sum_{i \in I} \ln f_{N_R^s}(N^i; \tilde{\mu}, \Sigma_a^i) \right) \tag{19}$$

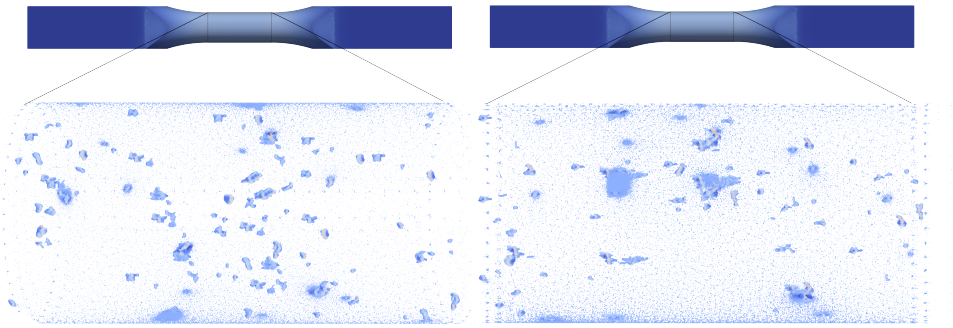

FIGURE 3 – Example of two generated synthetic specimens containing a combination of 20 random sub-volumes of pores. Both surface-breaking and in-volume pores are present.

Where N^i is the number of cycles to failure at an applied loading Σ_a^i. The expectation is taken over all realisations of the specimen with random meso-scale pore distributions. A Monte Carlo method is used to approximate this expectation over a finite number of porous specimen realisations (denoted as the set $\tilde{K}$) :

$$\mu = \arg\max_{\tilde{\mu}} \sum_{k\in\tilde{K}} \left(\sum_{i\in I} \ln f_{N_R^s}(N^i;\tilde{\mu},\Sigma_a^i) \right) \tag{20}$$

In practice, weights are added to the likelihood function. [1] A total of 30 synthetic specimens containing random distributions of pores, using the method detailed in the previous section (2.4) were generated for maximizing the likelihood function.

3 Numerical results

3.1 Uncertainty due to varying pore distributions and micro-heterogeneity

The modelled fatigue lifetime distribution models uncertainty due to two sources - micro-structural heterogeneity and meso-scale pores. Figure 4 shows the fit of the model for one synthetic porous specimen, keeping in mind the following considerations :

— Experimental fatigue data on real porous specimens consists of structures that fail after a finite number of cycles, and some specimens that did not break after 2.10^6 tested cycles. The number of specimens falling in the latter category is counted and reported at the 2.10^6 cycles mark followed by arrows and an ∞ sign, to denote possible failure in the event of future cycling, up until never failing at all (infinity).

— Numerical samples from the model are considered finite if below 2.10^6 cycles, any samples beyond this limit show a potential of higher lifetime. As there is no experimental data beyond 2.10^6 cycles, these samples are counted and reported at 2.10^6 cycles followed by arrows and an ∞ sign, to compare with the experimental data falling in this category.

1. The experimental fatigue data available for this study had a particularity : certain tested applied stress levels did not contain a lot of failure points. Therefore, weights (α_i) were added to the likelihood function. If I is the set of applied stresses and $\mathcal{J}$ is the set of all the specimens tested in a given stress level, and the number of failure points at a given applied stress level is n_i :

$$\mu = \arg\max_{\tilde{\mu}} \sum_{k\in\tilde{K}} \left(\sum_{i\in I} \sum_{j\in\mathcal{J}} \alpha_i \ln f_{N_{R,S}}(N^{i,j};\tilde{\mu},\Sigma_0^{k,e}(\Sigma_a^{i,j})) \right) \text{ where } \alpha_i = 1/n_i \tag{21}$$

TABLE 1 – Parameters of the micro-inclusion model identified on porous structures

Parameter	β (MPa)	m	A (MPa)
Value	2.92e9	3.90	8.95e8

— 30 numerical samples are shown per stress level, to compare the ratio of points at infinity. A ratio of infinite-to-total points of 33%, 46%, 70%, 90% and 96% is found numerically for each of the applied stress levels 40, 50, 60, 70 and 80 MPa, which is an excellent match with the experimental ratios of 40%, 50%, 100%, 100% and 100% respectively. The differences may be explained by the limited number of fatigue experiments conducted for each stress level.

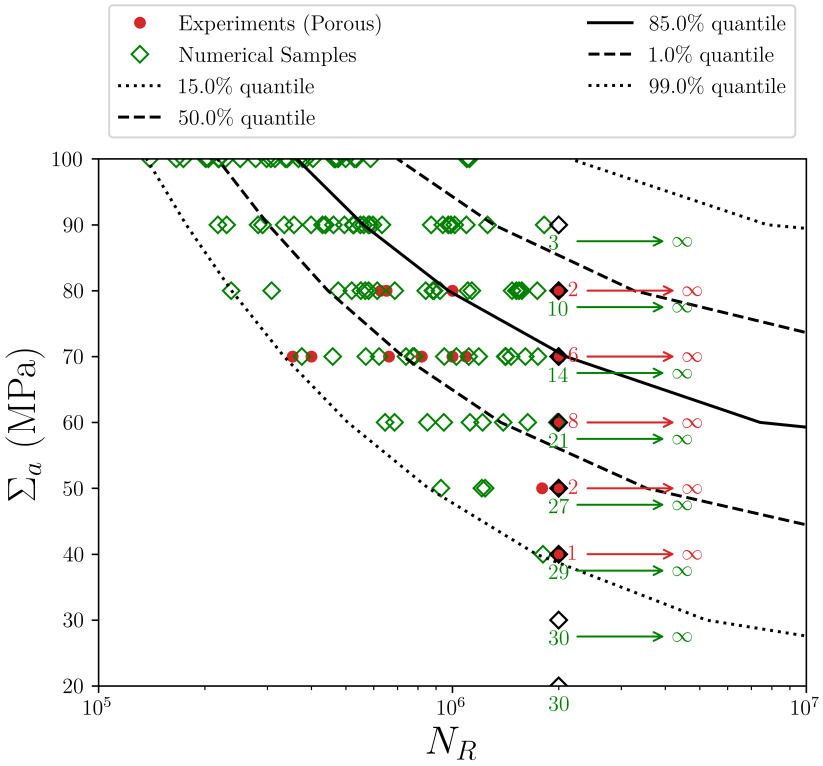

FIGURE 4 – Wohler curve for a synthetic porous specimen (black) and failure sampling (green). The parameters were obtained via an MLE using 30 synthetic porous specimens on the experimental fatigue data (red points). No significant change in the Wohler curve was found when changing to new pore distributions in the same specimen geometry, due to very similar stress distributions between the synthetic specimens.

The parameters of the micro-inclusion model identified on porous structures are summarized in table 1. No change in the Wohler curve was found when changing to new porous specimens of the same dimensions, which may be explained by similar stress distributions between porous specimens of the same dimensions. In other words, all the uncertainty in fatigue lifetime is attributed to the micro-inclusion model. To see an effect of the pore distribution, two cases may be studied : comparison of several smaller specimens with a lower number of pores, or a comparison of a thinner specimens of the same volume as the original specimen, the latter of which is demonstrated in the following section.

3.2 Pore-surface interactions : Lifetime of thin specimens

Thinner specimens (with the same volume as a given specimen) have higher pore-surface interaction, and thus have a lower lifetime. The fatigue model developed here demonstrates this result thanks to the pore distribution being modelled. Figure 5 shows a consistent decrease in the fatigue lifetime of a thinner specimen, transformed to have more surface area to volume ratio, while keeping the same volume as the original specimen.

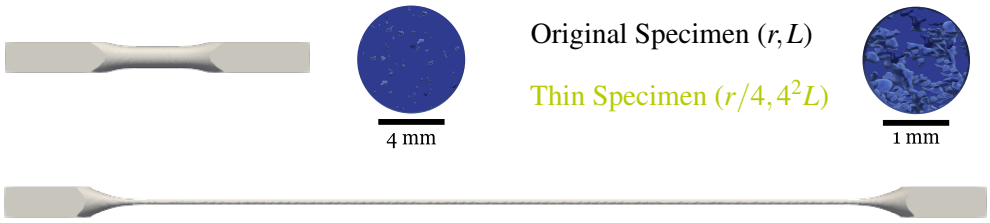

(a)

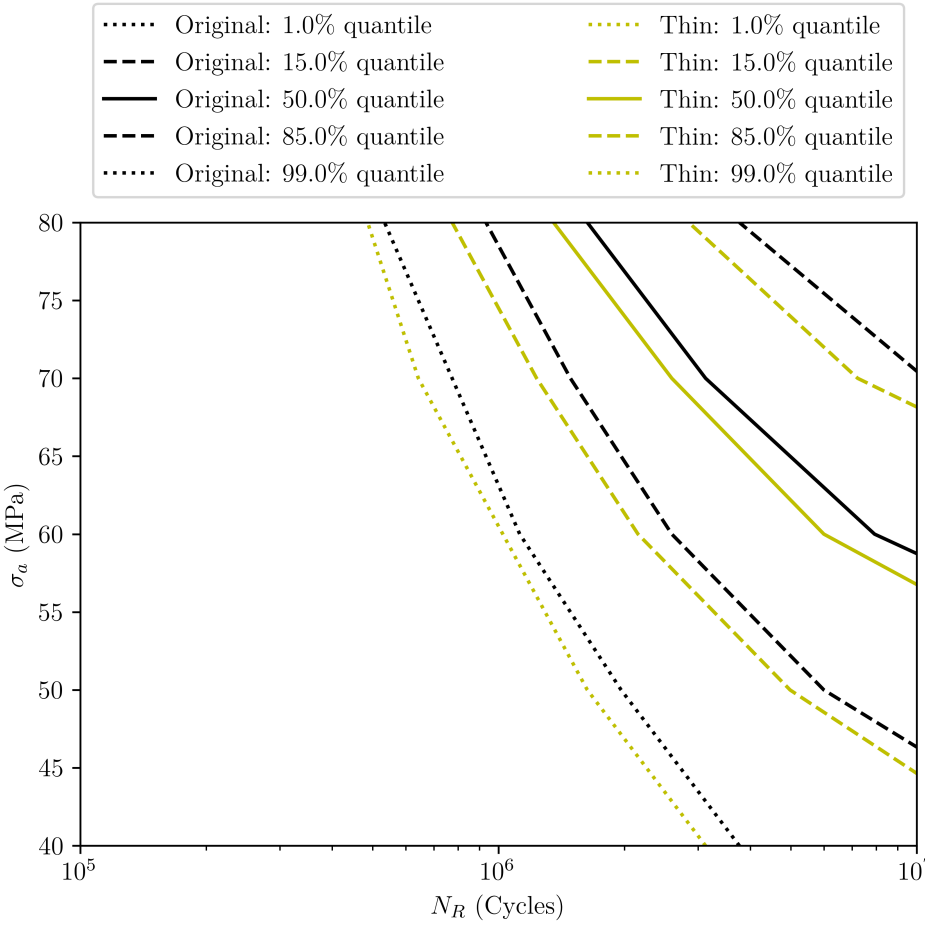

(b)

FIGURE 5 – (a) Illustration of two specimens : a specimen with radius r and length L, and a thin specimen, transformed but with the same volume as the original specimen (b) Resulting fatigue lifetime in the original and thin specimens

4 Références bibliographiques

Références

[1] Viet-Duc Le, Franck Morel, Daniel Bellett, Nicolas Saintier, and Pierre Osmond. Multiaxial high cycle fatigue damage mechanisms associated with the different microstructural heterogeneities of cast aluminium alloys. *Materials Science and Engineering : A*, 649 :426–440, 2016.

[2] Haijun Gong, Khalid Rafi, Hengfeng Gu, Thomas Starr, and Brent Stucker. Analysis of defect generation in ti–6al–4v parts made using powder bed fusion additive manufacturing processes. *Additive Manufacturing*, 1-4 :87–98, 2014. Inaugural Issue.

[3] Cédric Doudard, Sylvain Calloch, François Hild, Philippe Cugy, and André Galtier. Identification of the scatter in high cycle fatigue from temperature measurements. *Comptes Rendus Mécanique*, 332(10) :795–801, 2004.

[4] C. Doudard, S. Calloch, P. Cugy, A. Galtier, and F. Hild. A probabilistic two-scale model for high-cycle fatigue life predictions. *Fatigue & Fracture of Engineering Materials & Structures*, 28(3) :279–288, 2005.

[5] Anthony Ezanno, Cédric Doudard, Sylvain Calloch, and Jean-Loup Heuzé. A new approach to characterizing and modeling the high cycle fatigue properties of cast materials based on self-heating measurements under cyclic loadings. *International Journal of Fatigue*, 47 :232–243, 2013.

[6] F. Curà, G. Curti, and R. Sesana. A new iteration method for the thermographic determination of fatigue limit in steels. *International Journal of Fatigue*, 27(4) :453–459, 2005.

[7] G La Rosa and A Risitano. Thermographic methodology for rapid determination of the fatigue limit of materials and mechanical components. *International Journal of Fatigue*, 22(1) :65–73, 2000.

[8] Junling Fan, Xinglin Guo, and Chengwei Wu. A new application of the infrared thermography for fatigue evaluation and damage assessment. *International Journal of Fatigue*, 44 :1–7, 2012.

[9] A. Ezanno, C. Doudard, S. Calloch, T. Millot, and J.-L. Heuzé. Fast characterization of high-cycle fatigue properties of a cast copper–aluminum alloy by self-heating measurements under cyclic loadings. *Procedia Engineering*, 2(1) :967–976, 2010. Fatigue 2010.

[10] Lorenzo Bercelli, Sylvain Moyne, Matthieu Dhondt, Cédric Doudard, Sylvain Calloch, and Julien Beaudet. A probabilistic approach for high cycle fatigue of wire and arc additive manufactured parts taking into account process-induced pores. *Additive Manufacturing*, 42 :101989, 2021.

[11] Driss El Khoukhi, Franck Morel, Nicolas Saintier, Daniel Bellett, Pierre Osmond, Viet-Duc Le, and Jérôme Adrien. Experimental investigation of the size effect in high cycle fatigue : Role of the defect population in cast aluminium alloys. *International Journal of Fatigue*, 129 :105222, 2019.

[12] R. Desmorat, A. Kane, M. Seyedi, and J.P. Sermage. Two scale damage model and related numerical issues for thermo-mechanical high cycle fatigue. *European Journal of Mechanics - A/Solids*, 26(6) :909–935, 2007.

[13] A. Palchoudhary, V. Maurel, C. Ovalle, and P. Kerfriden. A fast neuber-type finite element simulator to enable deep-learning-based fatigue life predictions from thermographic data. In *Congrès Français de Mécanique, Nantes*, 2022.

[14] H. Kitagawa. Applicability of fracture mechanics to very small cracks or the cracks in the early stage. In *Proceedings of 2nd ICM, Cleveland*, pages 627–631, 1976.

[15] Viet-Duc LE, Franck Morel, Daniel Bellett, Etienne Pessard, Nicolas Saintier, and Pierre Osmond. Microstructural-based analysis and modelling of the fatigue behaviour of cast al-si alloys. *Procedia Engineering*, 133 :562–575, 2015. Fatigue Design 2015, International Conference Proceedings, 6th Edition.